Droplet Combustion of 87 Octane Gasoline and Comparison with n-Butanol

Special Investigations in MAE (MAE 6900)
In Partial Fulfillment of the Requirements for the Degree of
Master of Engineering

Advisor: C. Thomas Avedisian
Ph.D. Student Supervisor: Yuhao Xu
Sibley School of Mechanical and Aerospace Engineering
Cornell University

Zain Ali

5/19/2014

Abstract

This study reports experimental results concerning the droplet combustion characteristics of a commercial 87 octane-rated unleaded gasoline and compares them to the combustion characteristics of n-butanol. N-butanol has emerged as a potential competitor to ethanol for blending with gasoline because of its higher cetane number, lower vapor pressure, and higher miscibility. Therefore, it is important to compare the combustion dynamics of butanol and gasoline. This study does this from the perspective of single isolated droplets as components to a full spray.

Using the fundamental droplet combustion configuration of near spherical symmetry as promoted by low gravity in the standard ambience, this work reports experimental data for gasoline and n-butanol with initial an droplet diameters in the range of 0.52mm to 0.63mm. A free-fall facility was used to create low gravity. The facility contained a sealed chamber with the deployed droplets anchored to a very small diameter (14 μm) SiC fiber in the internal gas environment (room temperature air in the present investigation). Two high energy spark electrodes placed on either side of the droplet are used for ignition. High resolution digital video images are obtained of the droplet burning history. The video images are used to obtain quantitative data using computer imaging analyses software. The data reported include the evolution of the droplet (D), soot shell (D_s), and flame (D_f) diameters.

The results show that the evolution of the droplet diameter of n-butanol was almost identical to pure gasoline, though the flame stand-off ratio of gasoline was somewhat higher compared to n-butanol. The remarkable similarity of the burning rate of butanol and gasoline suggests that blends of these two fuels may perform similarly to pure gasoline. Such an outcome would be significant for its implication to reduce the consumption of petroleum-based fuels by blending gasoline with butanol.

Nomenclature

D: droplet diameter (mm)

D_0: initial diameter of droplet (mm)

D_f: flame diameter (mm)

D_s: soot shell diameter (mm)

t: time (s)

K_0: burning rate value (mm^2/s)

H = height of the ellipse

W= width of the ellipse

SSR: soot stand-off ratio

FSR: flame stand-off ratio

1. Introduction:

The extensive use of liquid fuels in transportation systems has made them a dominant source of energy. The emergence of sustainable energy technologies might lighten the burden on fossil fuels. A strategy to reduce the use of petroleum fuels is to blend them with suitable alternatives that have similar physical and chemical properties. For this particular reason, bio-fuels are being studied extensively. Immediate benefits can be derived from the understanding of the combustion performance of systems powered by conventional liquid fuels and consequently this can help identity different blends that might be used.

The unique properties of butanol (C_4H_9OH, boiling point at 117.4^oC) as a fuel, along with decreased volatile organic compound emission [1], has made butanol an option worth evaluating. Prior studies have found favorable results when butanol has been blended with gasoline and in some cases butanol provides significant benefit over ethanol/gasoline blends. Szwaja and Naber [2] were able to determine that n-butanol and n-butanol blends combust comparably to that of gasoline. Additionally, butanol/gasoline blends barely affect the drivability performance over a broad range of butanol concentrations [3]. Moreover, butanol, has a higher energy content than ethanol and so is an attractive alternative to ethanol (C_2H_6O, boiling point at 78.37^oC) [4].

This project examines the burning of gasoline and butanol from the perspective of isolated droplets. Interest in this configuration has existed since the earliest days of combustion processes and continues to the present time [5-9]. Our desire is to better understand combustion of fuel droplets and examine the different characteristics, such as combustion chemistry, fuel evaporation processes and the transient effects the droplet exhibits. To do this, the study of the base case of spherical symmetry is ideal. The spherical symmetric configuration promotes one dimensional transport, and the data obtained is easier to model than that of droplets in a convective flow field. The configuration is achieved by burning test droplets in a stagnant ambience, restricting their movement(by mounting them onto SiC fibres of diameter 14μm), and performing the experiments in a low gravity environment(order of 10^{-4} of Earth's normal gravity). This environment is achieved by doing the experiments in a free-fall facility that incorporates a drag shield. Consequently these conditions result in low Reynolds and Rayleigh's number which in turn promotes spherical gas symmetry in the droplet burning process. Figure 1 shows the droplet flame structure for this configuration. The figure depicts the droplet, a soot shell and a flame in the absence of external convection. The experiments are carried out in a

facility that promotes spherical symmetry of the droplet burning process by reducing the effects of convection. The basic goals in these experiments might include the evolution of the droplet diameter, the burning rate of the droplet, in addition to the flame and soot-shell standoff ratios.

This paper concerns studying the combustion characteristics of gasoline (87 octane) under conditions that promote spherical symmetry. D_0 will range from 0.52 mm to 0.63 mm. This experiment recorded the droplet burning history at ambient conditions of atmospheric pressure and room temperature air.

2. Experimental Method:

The experiment is designed to promote spherical droplet flames by minimizing the influence of external convection. Buoyancy and gravity effects were minimized by carrying out the experiment in a free-fall facility. The experimental design and procedures follow the description given in [10]. A brief description is given here.

With reference to Figure 2, the fiber support structures are placed in a crossing pattern and the droplets are directed at the intersection of the crossing of the fibers. A piezoelectric generator (HP 214B) is used to direct fuel droplets onto two fibers (14μm), until the droplet reaches the desired size. The droplet, generator, electrodes and support fiber mounts are secured in a sealed chamber containing room temperature air at atmospheric pressure. The sealed chamber and cameras are then released into free fall over a 7.6m distance to give an experimental time of 1.2 s of low gravity (i.e., 10^{-4} of Earth's normal gravity). Droplet ignition is delayed after free-fall begins to reduce influences of vibration associated with release of the instrumentation package. To reduce spark disturbances, the lowest possible energy that achieves ignition was employed. The time sequence of package release, spark activation, and electrode retraction is coordinated by a multichannel digital signal composer (QC-9618). The droplet burning process is recorded by two cameras in perpendicular views as shown in Figure 2.

3. Data Analysis

To obtain quantitative measurements of the evolution of the droplet, soot shell and flame diameters, the video imaging of the droplet burning process is used. Two methods are available to measure the diameters. One is an automated process as described in [11], and the other is a manual procedure using commercial software (Image-Pro v6.3). Due to the sooty nature of the fuel the manual method was employed. The process involves placing an ellipse around the droplet and the soot-shell and then calculating D as $= (H \times W)^{0.5}$. A sample of how the ellipse is place on the droplet and the soot shell is shown in Figure 3. Image Pro returns W and H in pixels. The pixels are converted to millimeters using an image from a calibration ball. The flame dimension is measured by using CorelDRAW software. As shown in Figure 4, an ellipse is placed around the outer blue flame and CorelDRAW provides the W and H. D_f is then obtained as $D_f = (W \times H)^{0.5}$.

3.1 Quantitative Data

The evolution of the droplet size, along with soot shell dynamics, and spherical droplet flame for gasoline for the indicated value of D_0 is shown in Figure 5. Figure 6 shows the evolution of the droplet size for the current runs of the gasoline with the indicated values of D_0. The coordinates in this figure are motivated from the classical theory of droplet combustion which shows that [6]

$$\left(\frac{D}{D_0}\right)^2 = 1 - K_0 * \frac{t}{D_0^2} \quad (1)$$

where the burning rate K_0 is

$$K_0 = -\left(\frac{d(\frac{D}{D_0})^2}{d(\frac{t}{D_0{}^2})}\right) \quad (2)$$

From eq. 1, the evolution of $(D/D_o)^2$ with t/D_0^2 should be linear, which is almost consistent with the trends in figure 6. In the remaining presentation of data we present the results in terms of this time coordinate, t/D_0^2.

The data for D_0=0.53mm gasoline and 0.56mm n-butanol come from previous studies, [10], [12] respectively , and are included for comparison. As can be seen in Figure 6, gasoline and n-butanol are almost identical to each other. Figure 7 shows the burning rates of gasoline and n-butanol. The burning rates conform over most of the burning history. Initially, the burning rates increase during the transient droplet heating process, but then are relatively constant.

Figure 5 shows the related images of the burning sequence of the gasoline droplet with the indicated D_0. The flame has a yellow inner core with a faint outer blue boundary. The yellow inner core is due to the soot incandescence while the blue zone suggest CH emissions. The two needle like glows on the side of the spherical flame are due to the interaction of the flame and the supporting fibers. The FSR, which is a relative measure of the position of the flame to the droplet, is shown in Figure 8. The FSR for the two present gasoline runs(D_0=0.62 mm and D_0= 0.63 mm) are almost identical, but D_o= 0.52 mm gasoline has a higher FSR. Additionally, butanol has a relatively lower FSR when compared to the current gasoline runs. Figure 9 shows the evolution of the flame diameter of gasoline and butanol. D_0=0.62 mm and D_0= 0.63 mm have an almost identical D_f which is to be expected since the initial diameter is almost the same. D_0=0.52 mm has a relatively lower D_f due to a lower initial diameter. In comparison to the

present runs of gasoline, n-butanol had a lower D_f. Additionally it was noticed that the FSR and the flame diameter for D_0= 0.53mm [10] is lower than that of the present gasoline runs. In order to investigate why the FSR of the present gasoline runs was higher than the previous measurements of gasoline, one of the runs from [12] was reanalyzed. Figure 10 and Figure 11, show that the analyzed data was underestimated. On reanalyzing the data it was realized that the previous gasoline run[10], had a similar flame diameter and FSR when compared to the D_0=0.52 mm. This is to be expected since both the runs have similar diameters.

The relative position of the soot shell to the droplet or the SSR is shown in Figure 12. In Figure 12, it can be seen that the SSR of the present gasoline runs is slightly higher than the 0.53mm gasoline [10]. One of the reasons for the different SSR can be attributed to the fact that in the averaged data of 0.53mm gasoline [10] one of the runs was considerably lower than the other two which in turn dragged the average down

4. Conclusion

The results in this report showed that the evolution of droplet diameter for n-butanol was almost identical to pure gasoline. Additionally, the flame diameter of the three gasoline runs was significantly higher than that of n-butanol, most likely due to the soot formation during the burning history of gasoline. Moreover, the flame stand-off ratio of the pure gasoline was considerably higher than that of pure n-butanol. Due to the findings of this experiment it would be interesting to repeat the experiment with a blend of gasoline and n-butanol. Depending on the concentration of the blend, the results would be expected to fall in between the results of pure gasoline and n-butanol.

Acknowledgements

This work was supported by the National Administration of Space and Aeronautics under Grant No. NNX08AI51G. The author thanks Dr. C. Thomas Avedisian for his support and useful discussion about the subject matter. The author appreciates the effort and guidance given by Mr. Yuhao Xu throughout the entirety of the project.

Works Cited

[1] Wu, M.; Wang, M.; Liu, J.; Huo, H. (2008). Assessment of Potential Life-Cycle Energy and Greenhouse Gas Emission Effects. *Biotechnology Progress , 24* (6), 1204-1214.

[2] Szwaja, S.; Naber, J. (2010). Combustion of n-butanol in a spark-ignition IC engine. *Fuel , 89* (7), 1573-1582.

[3] Yanowitz, J.; Christensen, E.; McCormick, R.L. (2011). *Utilization of Renewable Oxygenates as Gasoline Blending Components.* NREL. Cole Boulevard Golden: National Renewable Energy Laboratory.

[4] Fortman, J.; Chhabra, S.; Mukhopadhyay, A.; Chou, H.; Lee, T. S.; Steen, E.; et al. (2008). Biofuel alternatives to ethanol. *Trends in Biotechnology , 26* (7), 375-381.

[5] Godsave, G. (1953). Studies of the combustion drops in a fuel spray- the burning of single drops of fuel. *Proceedings of the Combustion Institute , 4* (1), 818-830.

[6] Turns, S. (2000). An Introduction to Combustion. New York: Mcgraw-Hill.

[7] Jackson, G. S.; Avedisian, C. T. (1994). The effect of initial diameter in spherically symmetric droplet combustion of sooting fuels. *Proceedings: Mathematical and Physical Sciences , 446* (1927), 255-276.

[8] Jackson, G. S.; Avedisian, C. T.; Yang, J. C. (1992). Observations of Soot in Droplet Combustion at Low Gravity: Heptane and Heptane/Monochloroalkane Mixtures. *International Journal of Heat and Mass Transfer , 35* (8), 2017-2033.

[9] Avedisian, C. T. (2000). Recent advances in soot formation from spherical droplet flames at atmospheric pressure. *Journal of Propulsion and Power , 16* (4), 628-635.

[10] Liu, Y. C.; Avedisian, C. T. (2012). A comparison of the spherical flame characteristics of sub-millimeter droplets of binary mixtures of n-heptane/iso-octane and n-heptane/toluene with a commercial unleaded gasoline. *Combustion and Flame , 159*, 770-783.

[11] Dembia, C. L.; Liu, Y. C.; Avedisian, C. T. (2012). Automated Data Analysis For Consecutive Images From Droplet Combustion Experiments. *Image Analysis and Stereology , 31*, 137-148.

[12] Fahd, E.; Liu, Y. C.; Avedisian, C. T.; Dryer, F.; Farouk, T. *A Detailed Numerical Simulation of Spherically Symmetric n-Butanol Droplet Combustion and Comparisons with Experimental Data. Proc. Comb. Inst. 35, Inpress (2014)*

Appendix A: Figures

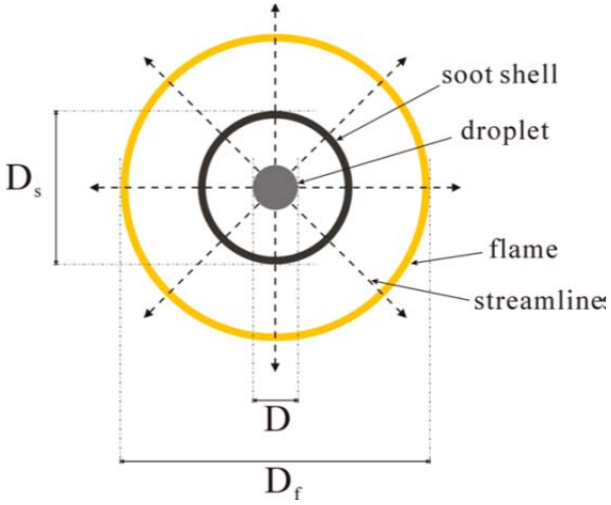

Figure 1: Schematic of a spherically symmetric droplet flame structure. [10]

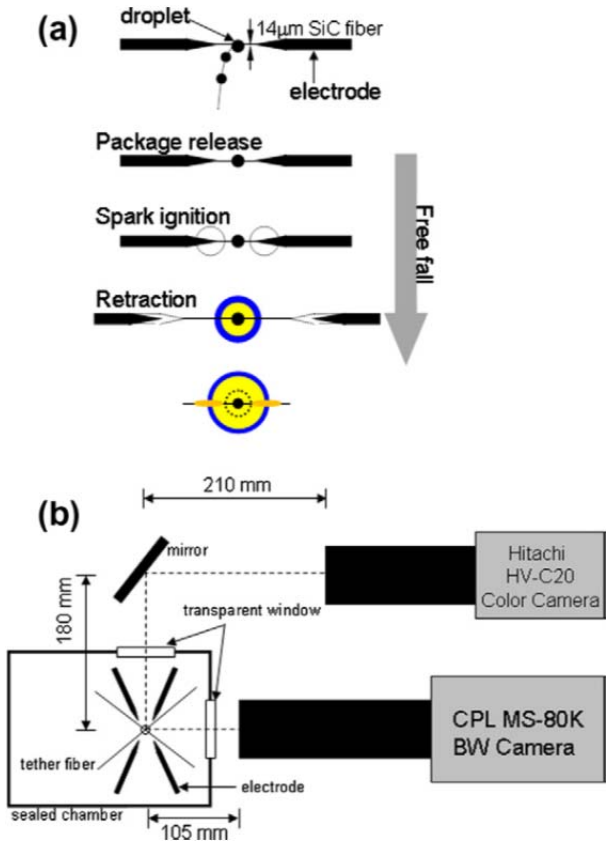

Figure 2: (a) schematic of procedure; (b) layout of package. [10]

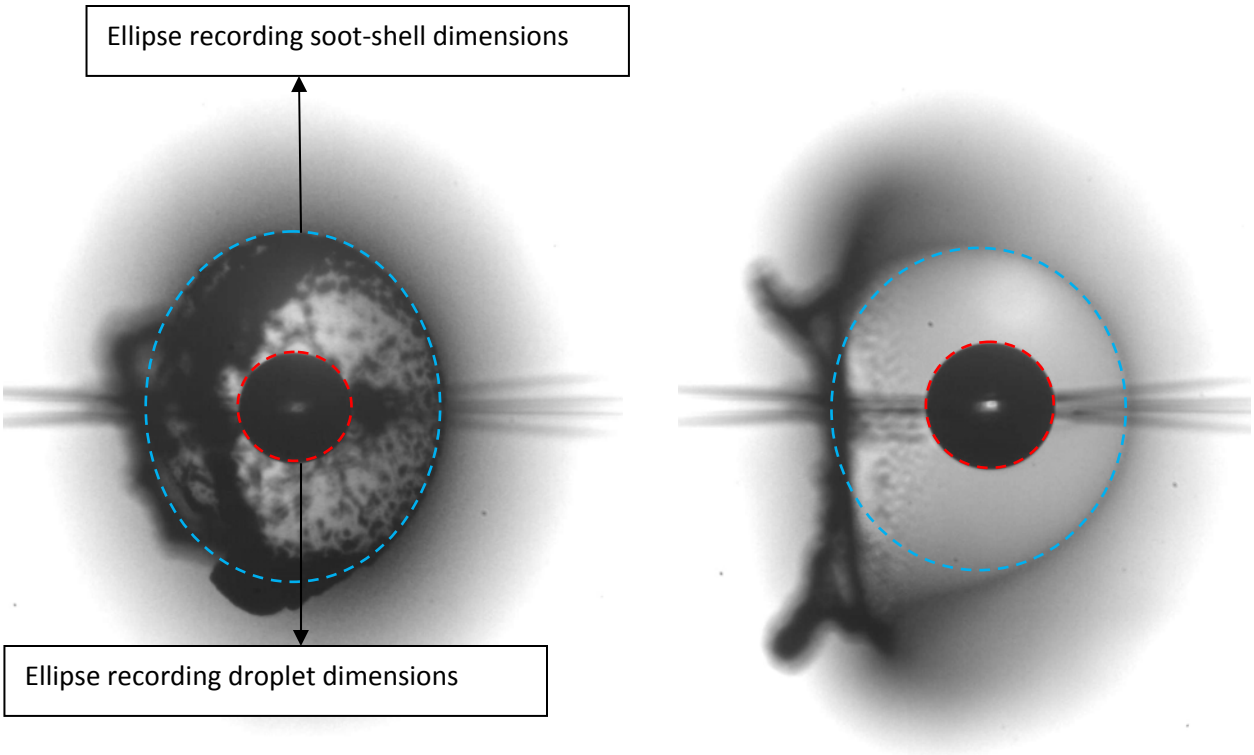

Figure 3: Selected BW images showing how the droplet and soot-shell dimensions were recorded.

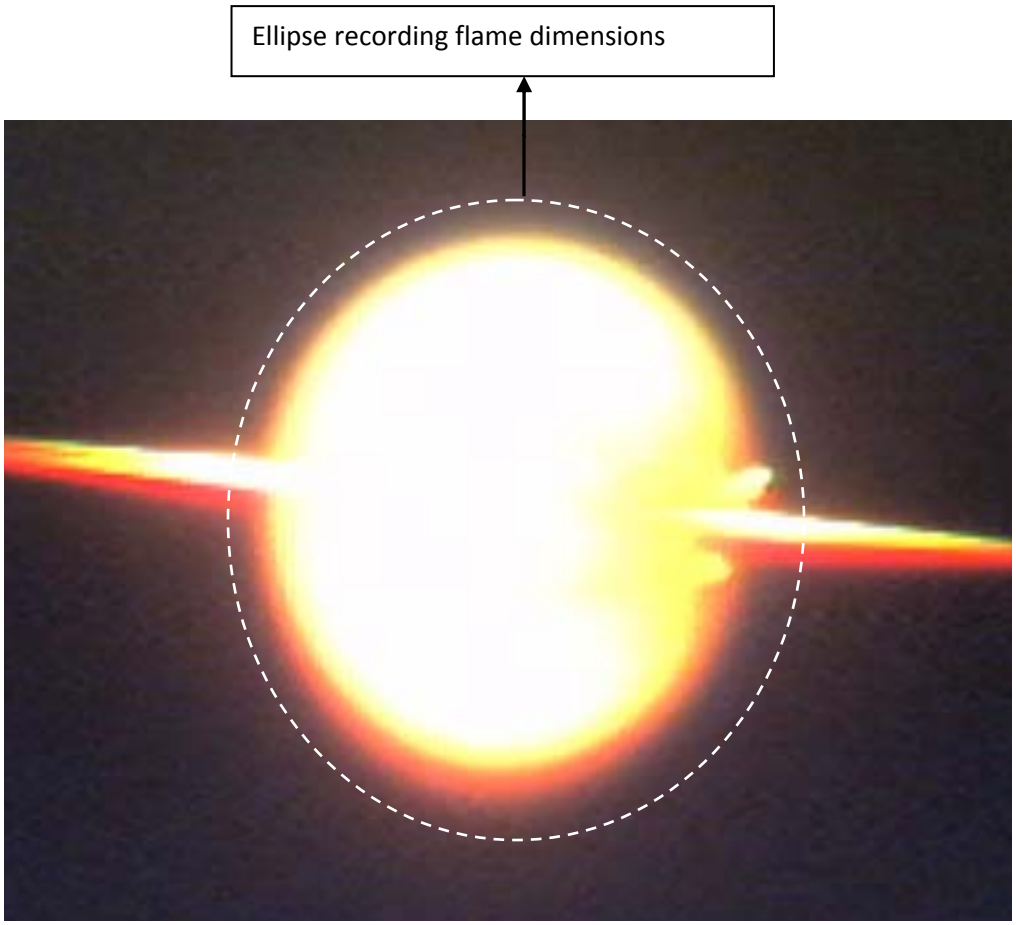

Figure 4: Selected color image showing how the flame dimensions were recorded.

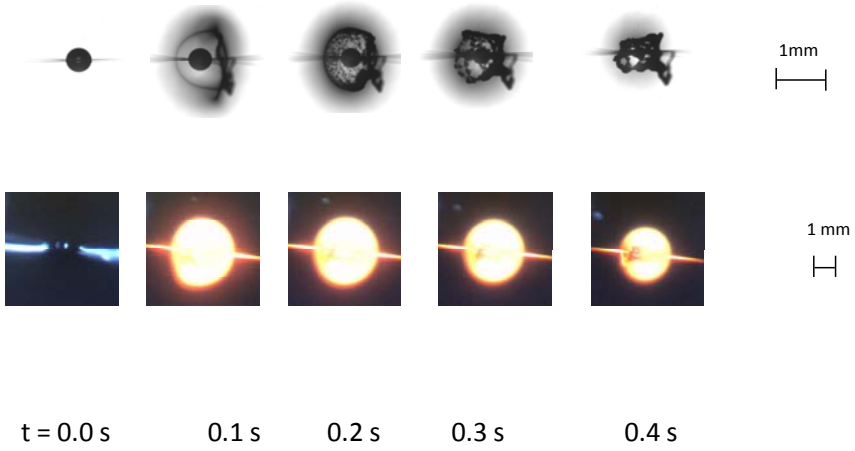

Figure 5: Selected BW and color images showing evolution of droplet size, soot structure dynamics and evolution of spherical droplet flame for gasoline with D_0= 0.52 mm

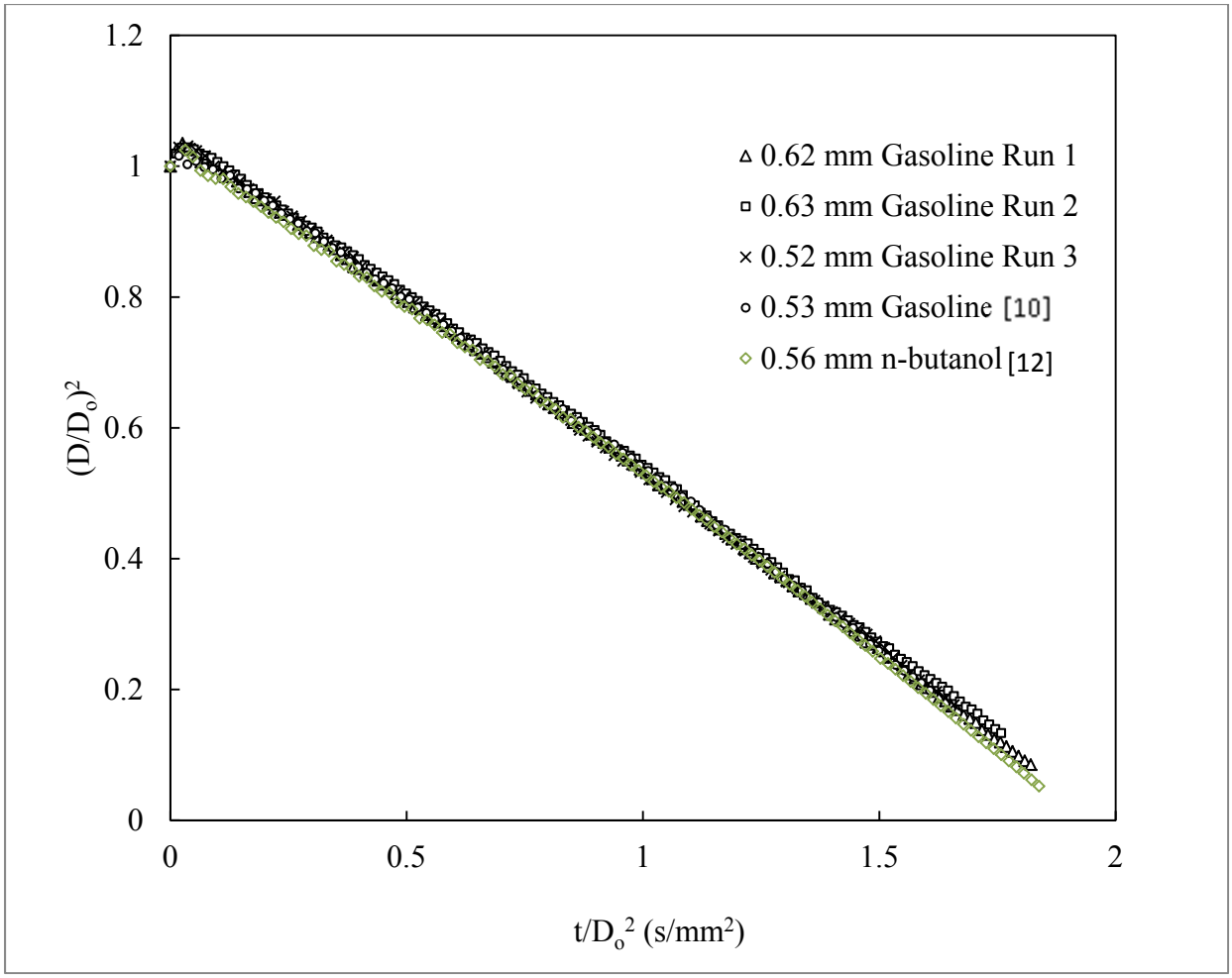

Figure 6: Evolution of droplet diameters for three runs of gasoline. Also shown are data for 0.53mm gasoline [10] and 0.56mm n-butanol [12].

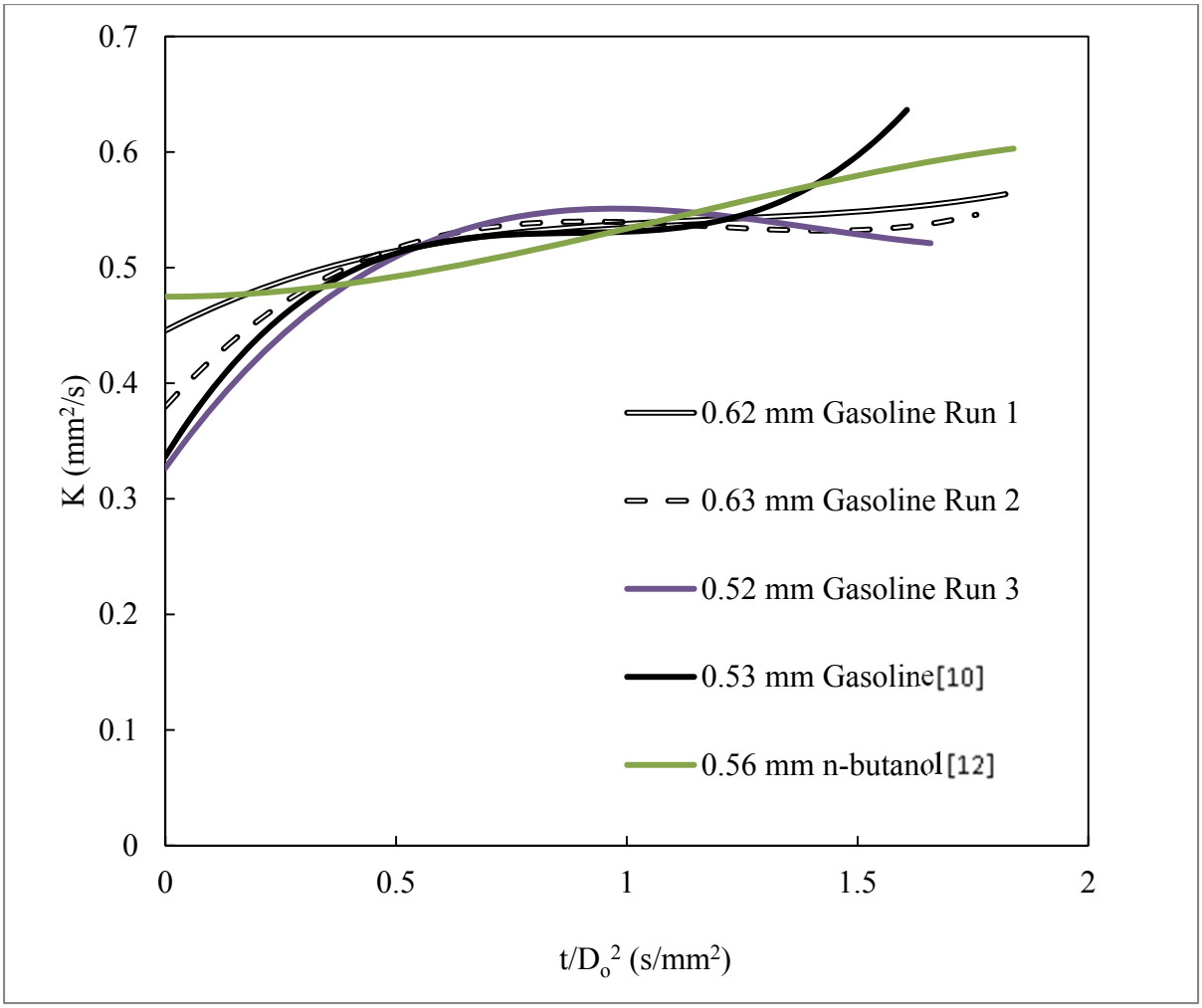

Figure 7: Burning rates as computed from a 4th order polynomial of the data in Figure 6.

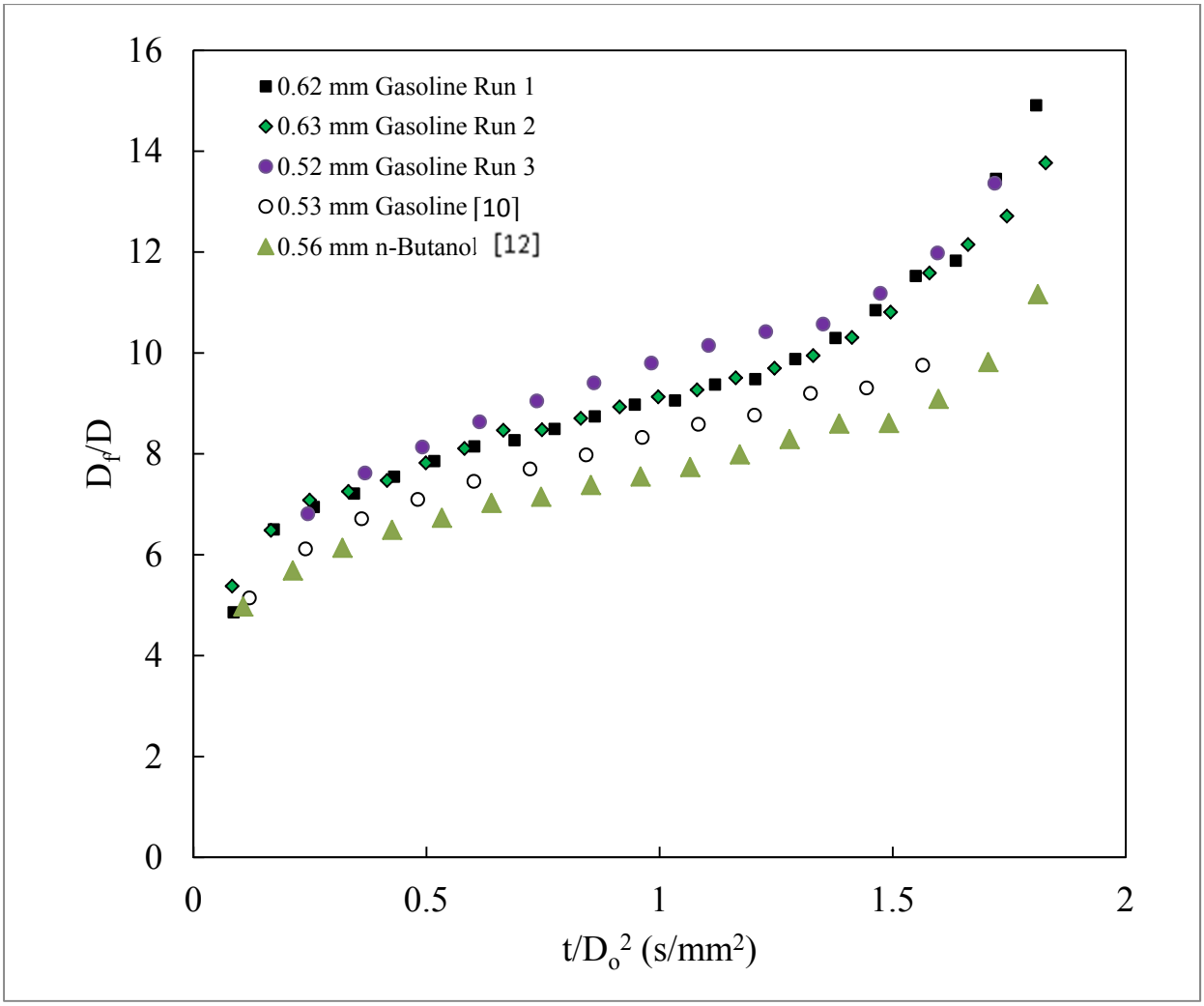

Figure 8: Evolution of FSR of the fuel investigated and compared to 0.53mm gasoline [10] and 0.56mm n-butanol [12].

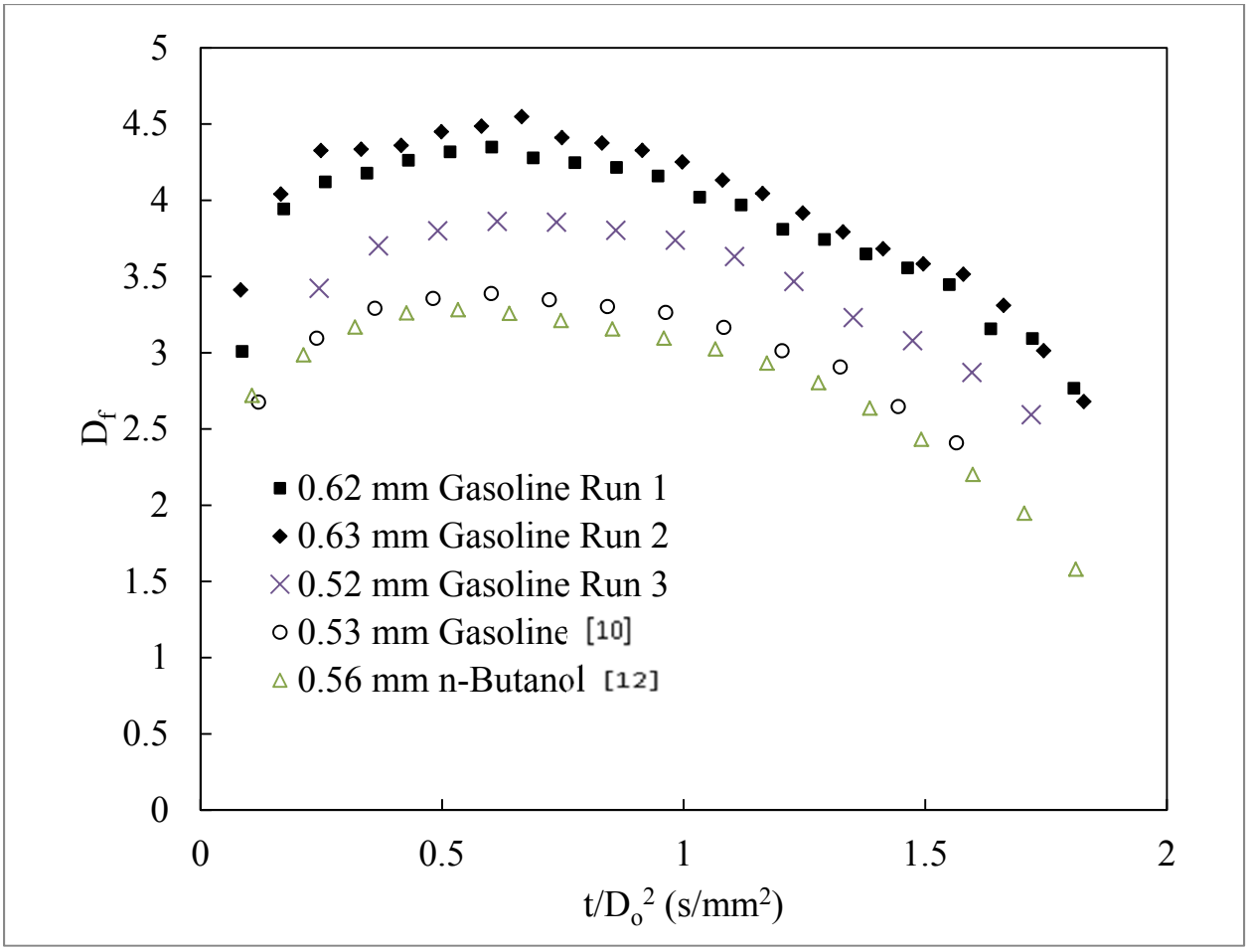

Figure 9: Evolution of the flame diameter for the fuel investigated and compared to 0.53mm gasoline [10] and 0.56mm n-butanol [12].

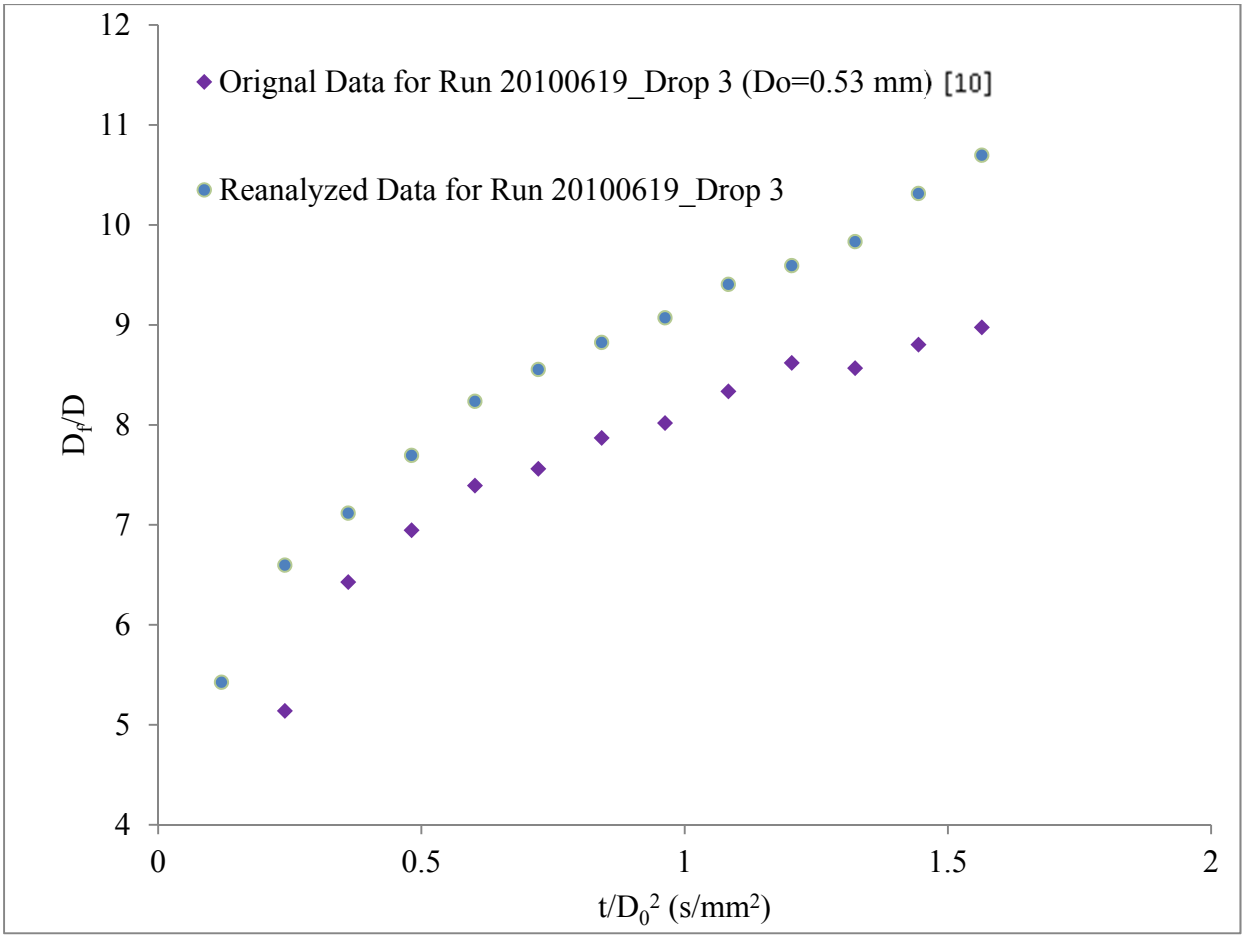

Figure 10: Reanalyzed FSR Data for Gasoline Run 20100619_Drop 3 [10].

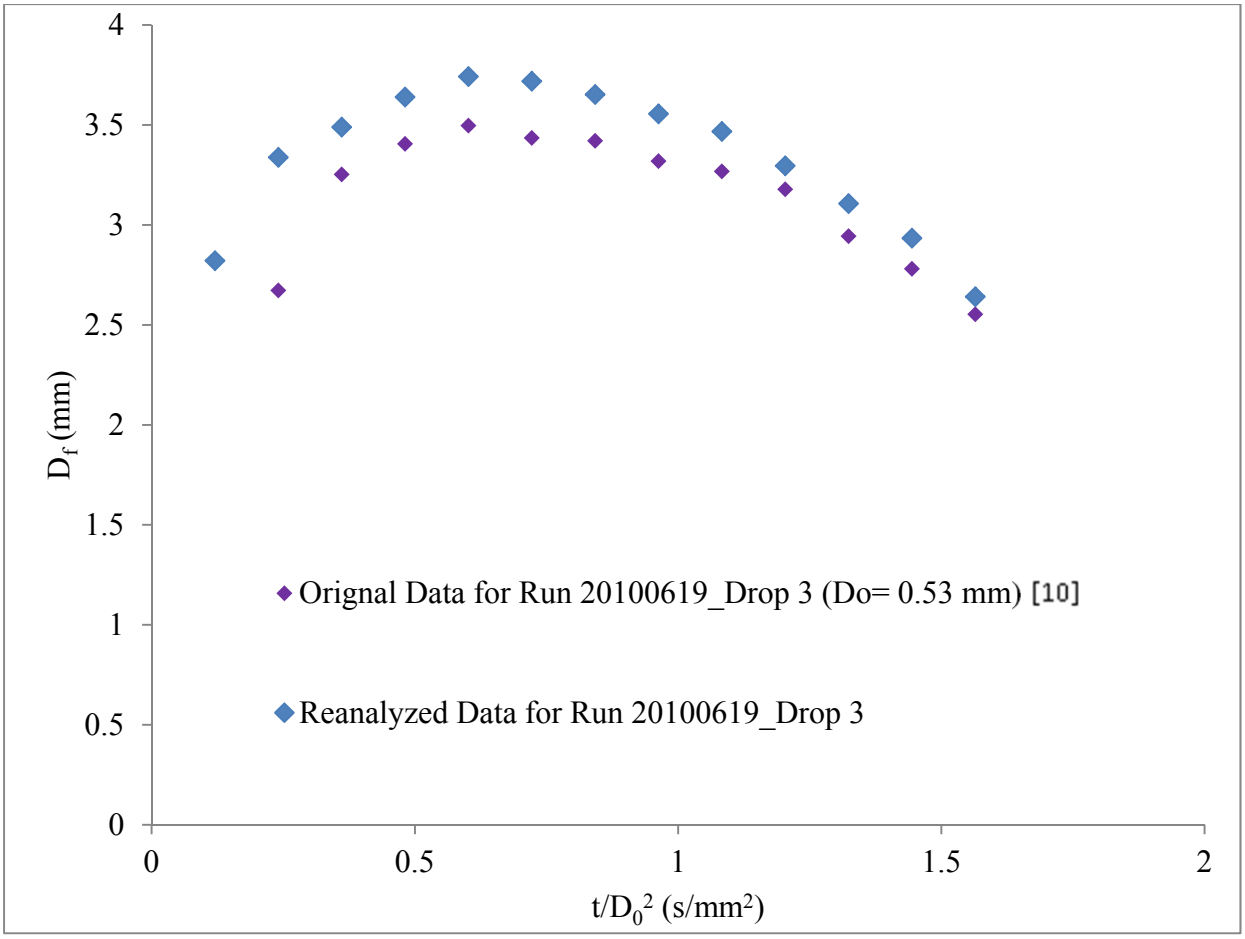

Figure 11: Reanalyzed Flame Diameter Data for Gasoline Run 20100619_Drop 3 [10].

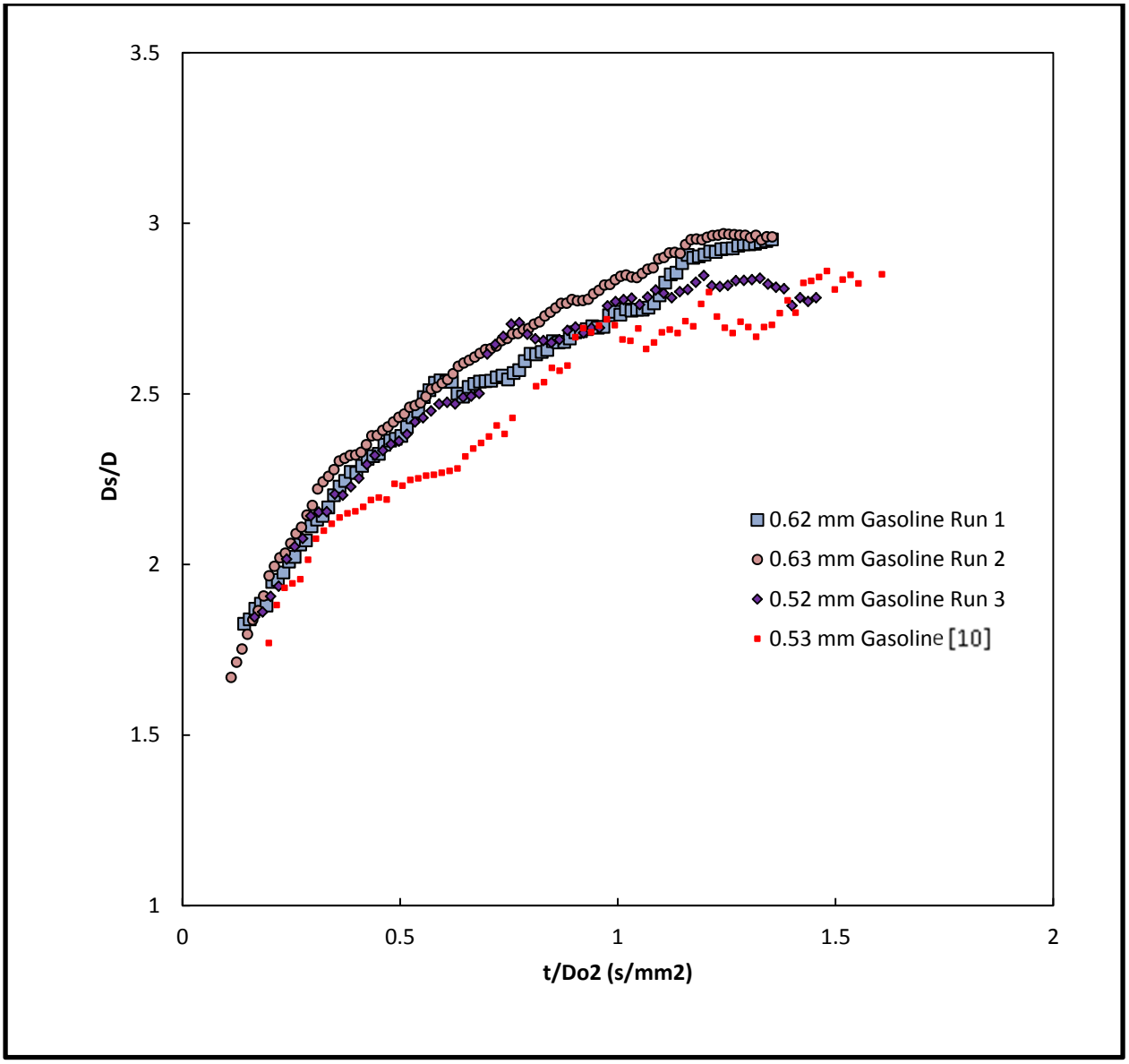

Figure 12: SSR for the fuel investigated and compared to 0.53mm gasoline [10].